Climate Dynamics (2001) 17: 905–922

M. Webb · C. Senior · S. Bony · J.-J. Morcrette

Combining ERBE and ISCCP data to assess clouds in the Hadley Centre, ECMWF and LMD atmospheric climate models

Received: 23 January 2000 / Accepted: 24 January 2001

Abstract This study compares radiative fluxes and cloudiness fields from three general circulation models (the HadAM4 version of the Hadley Centre Unified model, cycle 16r2 of the ECMWF model and version LMDZ 2.0 of the LMD GCM), using a combination of satellite observations from the Earth Radiation Budget Experiment (ERBE) and the International Satellite Cloud Climatology Project (ISCCP). To facilitate a meaningful comparison with the ISCCP C1 data, values of column cloud optical thickness and cloud top pressure are diagnosed from the models in a manner consistent with the satellite view from space. Decomposing the cloud radiative effect into contributions from low-medium- and high-level clouds reveals a tendency for the models' low-level clouds to compensate for underestimates in the shortwave cloud radiative effect caused by a lack of high-level or mid-level clouds. The low clouds fail to compensate for the associated errors in the longwave. Consequently, disproportionate errors in the longwave and shortwave cloud radiative effect in models may be taken as an indication that compensating errors are likely to be present. Mid-level cloud errors in the mid-latitudes appear to depend as much on the choice of the convection scheme as on the cloud scheme. Convective and boundary layer mixing schemes require as much consideration as cloud and precipitation schemes when it comes to assessing the simulation of clouds by models. Two distinct types of cloud feedback are discussed. While there is reason to doubt that current models are able to simulate potential 'cloud regime' type feedbacks with skill, there is hope that a model capable of simulating potential 'cloud amount' type feedbacks will be achievable once the reasons for the remaining differences between the models are understood.

M. Webb (✉) · C. Senior
Hadley Centre for Climate Prediction and Research,
The Met Office, London Road,
Bracknell, Berkshire RG12 2SY, UK
E-mail: mjwebb@meto.gov.uk

S. Bony
MIT & LMD/CNRS, Department of Earth,
Atmospheric and Planetary Sciences, Room 54-1721,
77 Massachusetts Avenue, Cambridge, MA 02139, USA

J.-J. Morcrette
European Centre for Medium-range Weather Forecasts,
Reading, Berkshire RG2 9AX, UK

1 Introduction

Clouds play an important role in climate, not only because they significantly modify the distribution of the shortwave and longwave radiation absorbed and emitted by the Earth, in turn affecting temperature, humidity and the general circulation, but also because they are themselves sensitive to these changes. Consequently, clouds have the potential to modify the response of the climate system to anthropogenic forcing through cloud radiative feedbacks. Differences between cloud feedbacks in climate models are a major contributing factor to the uncertainty in the models' responses to climate forcing (e.g. Roeckner et al. 1987; Le Treut and Li 1991; Senior and Mitchell 1993).

Senior (1998) points out that while many studies (e.g. Cess et al. 1990) of cloud feedbacks in models focus on changes in cloud radiative forcing (Harrison et al. 1990), the differences between the responses of different models can only be understood when changes in cloud properties (such as the 3-D distribution of cloud amount, in-cloud albedo, in-cloud emissivity) are also examined and related to different physical assumptions in the models.

If we are to have confidence in predictions from climate models, a necessary (although not sufficient) requirement is that they should be able to reproduce the observed present-day distribution of clouds and their associated radiative fluxes. Again, an unambiguous link to the physical assumptions in models can only be made if the validation goes beyond that of the models' simulation of radiative fluxes at the top-of-the-atmosphere, to assess the various aspects of the cloud simulations that control these fluxes, those at the surface and also

the radiative atmospheric heating rates. These quantities would ideally include the three dimensional distribution of cloud fraction, ice and liquid water paths and particle/droplet size distributions. While direct observations of all of these parameters are not currently available, existing datasets contain related information that can be used to constrain the models' clouds further than is possible using a single observational dataset alone.

Data products from the International Satellite Cloud Climatology Project (ISCCP, Rossow and Schiffer 1991) provide retrievals of cloud amount, cloud optical thickness and cloud top pressure with high temporal resolution. The purpose of this study is to illustrate new methods for combining the data from ISCCP and from ERBE (the Earth Radiation Budget Experiment, Harrison et al. 1990). These methods are able to highlight problems with the simulation of clouds in climate models not apparent when ERBE data alone are used. The benefits of using a multi-model approach are demonstrated by applying the techniques to data from three models. Although it is not our primary aim to relate the errors highlighted to problems with the formulations of the specific models, these issues are discussed where they are thought to be of general interest.

In Sect. 2, the models, the observational data, and the methods used to compare them are described. In Sect. 3, ERBE data are used to characterise the main areas for concern in the models' simulations of longwave and shortwave cloud radiative effects. Section 4 compares the models' cloud distribution with the ISCCP data in selected areas, and errors in the radiative fluxes in these areas are related to the cloud errors identified. Section 5 assesses the models' ability to reproduce certain relationships between the observed cloud amount and radiative fluxes. A discussion follows in Sect. 6.

In the remainder of this work we will refer to the cloud radiative forcing diagnostic as the cloud radiative effect, following (Chen et al. 2000).

2 Model data and observations

The three climate models are compared with data from the Earth Radiation Budget Experiment (ERBE, Harrison et al. 1990) and the C1 products from the International Satellite Cloud Climatology Project (ISCCP,Rossow and Schiffer 1991).

The Hadley Centre model used was a development version of HadAM4, a climate configuration of the Hadley Centre Unified Forecast and Climate Model (cullen 1993). This version was run with a horizontal resolution of 3.75° longitude and 2.5° latitude, and incorporated the following changes with respect to its predecessor, HadAM3 (Pope et al. 2000). Vertical resolution was enhanced in the upper troposphere, raising the total number of levels from 19 to 30 (Pope et al. 2001). The radiative effects of non-spherical ice particles were introduced (Kristjánsson et al. 1999). A cloud area parametrisation was introduced so as to allow clouds to fill only part of the vertical thickness of a model layer (Cusack personal communication). A new mixed-phase precipitation scheme (Wilson and Ballard 1999), based on the scheme of Rutledge and Hobbs (1983), introduced a prognostic equation for cloud ice, and calculates exchanges between liquid, ice and water vapour using physically based transfer terms. A scheme to treat the radiative effects of anvil cirrus in deep convective systems was introduced (Gregory 1999). The threshold relative humidity for diagnosis of cloud was parametrised as a function of horizontal variability resolved by the climate model (Cusack et al. 1999). A non-local boundary layer scheme was also introduced (Martin et al. 2000), which includes an explicit entrainment parametrisation (Lock 1998). The new scheme was accompanied by an increase in boundary layer resolution, raising the total number of vertical levels to 38. A new formulation for the cloud fraction was introduced to represent skewness in the subgrid distribution of total water, giving closer agreement with the in-situ observations presented in Wood and Field (2000) (Cusack personal communication) Also, the Barker (1996) parametrisation for the radiative treatment of cloud inhomogeneity in the shortwave and longwave parts of the spectrum was introduced (Cusack personal communication).

The ECMWF model used in this study was the cycle 16r2 version of the ECMWF forecast model, operational during the summer of 1996. It was run at a resolution of T63, with 31 levels in the vertical. It uses a reduced Gaussian grid corresponding to 1.875° at the equator and remaining equidistant in distance towards the poles (Hortal and Simmons 1991). All fields used herein are interpolated to a regular 2.5 by 2.5° grid (73 points of latitudes by 144 points of longitude). The physical package was the same as that used operationally until December 1997. Physical parametrisations particularly relevant for this study are the mass-flux convection scheme (Tiedtke 1989), the prognostic cloud scheme (Tiedtke 1993) and the radiation scheme (Morcrette 1991, 1993; Tiedtke 1996). The prognostic cloud scheme represents both stratiform and convective clouds and their time evolution is defined through two large-scale budget equations for cloud water content and cloud fractional cover. This scheme links the formation of clouds to large-scale ascent, diabatic cooling, boundary-layer turbulence and convective detrainment, and their dissipation to adiabatic and diabatic heating, turbulent mixing of cloud air with unsaturated environmental air, and precipitation processes. The results presented in the following sections are obtained with the scheme used operationally for global forecasts and analyses (Jakob 1994). It differs from Tiedtke's original formulation through a revised representation of the ice sedimentation after Heymsfield and Donner (1990).

The LMD model is Version 2.0 of the grid-point LMDZ GCM (Li 1999). The simulations are run here with a regular grid with 96 points in longitude and 73 in latitude and 19 sigma levels. The diurnal cycle is not activated in this version. A brief description of physical parametrisations relevant for this study follows.

Cloud water is predicted prognostically as a result of condensation, evaporation, advection and precipitation of cloud droplets. Convective processes are represented by a modified Kuo scheme combined with a moist adiabatic adjustment (MAA) scheme. Condensation associated with non-convective processes is handled by a statistical scheme that allows condensation to occur before saturation is reached at the large-scale. A uniform probability distribution function (PDF) is used to describe the sub-grid variability of the total water within the grid box (Le Treut and Li 1991). The half-width of the distribution is taken to be proportional to the total water amount within the grid box. The cloud fraction is diagnosed as the fraction of the grid box over which condensation occurs: this is 100% when associated with the MAA, the model time-step times the the total water vapour convergence over the water vapour amount necessary to saturate the unstable column when associated with the Kuo scheme, and the fraction deduced from the uniform PDF when associated with the non-convective condensation scheme. Convective and non-convective schemes are called in series in the model, the MAA being called first and the Kuo scheme last. The final cloud fraction used in the model and interacting with radiation is the maximum of the three cloud fractions diagnosed. In practice, this is equal to 100% as soon as the moist adiabatic adjustment is activated.

Precipitation of warm clouds is assumed to occur as the condensed water exceeds a critical threshold value, taking into account a characteristic time scale of 30 minutes (the time-step for physical parametrisations in the model). The precipitation rate of cold clouds is related to the terminal velocity of ice crystals (Heymsfield and Donner 1990).

The radiation scheme follows Fouquart and Bonnel (1980) for the solar, and Morcrette (1991) for the infrared. Cloud optical properties are diagnosed as functions of the cloud water path. The ice fraction of clouds is assumed to be a function of the gridbox mean temperature; it is zero above 273 K, unity below 258 K, and varies linearly with temperature between 258 K and 273 K.

The models were run to simulate a period of 18 months from May 1987 to October 1988, as a part of a European Community funded project on Cloud Feedbacks and Validation. They were forced with daily SSTs, calculated by linearly interpolating between the monthly mean observed SSTs supplied by AMIP, as is standard practice for such simulations. Monthly mean diagnostics were stored for the whole period, while instantaneous diagnostics were stored for the months of July 1987, January 1988 and July 1988, sampled every three hours from the Hadley Centre model, every six hours from the ECMWF model and every 24 hours from the LMD model.

The ISCCP C1 data were used, which comprise cloud occurrence in five categories of column cloud optical thickness and seven categories of cloud top pressure (35 in all), every three hours. Although the more recent D1 version of the ISCCP data is now available for the period in question, it is not expected that repeating the analysis using the D1 data would significantly affect our conclusions. This is because the largest differences between the two ISCCP versions (Doutriaux-Boucher and Seze 1998) are seen over land areas that are not considered in our analysis; the differences between the two ISCCP versions over the ocean regions under consideration here are small compared to those which are typically seen between the models and the retrievals in Sect. 4.

For the comparisons with the ISCCP data, special diagnostics were extracted from the models, in a manner similar to that employed by Yu et al. (1996), Del Genio et al. (1996) and Klein and Jakob (1999). This approach allows a more consistent comparison between model cloud and the ISCCP cloud products by taking into account the effects of overlapping clouds on the cloud distribution as seen from space. The procedure applied to the models in this study follows that of Klein and Jakob (1999), with the following exceptions:

1. A range of overlap assumptions are made so as to be consistent with the various assumptions of the radiation codes in the particular models. For the Hadley Centre model, this takes the form of a maximally overlapped convective cloud tower and anvil, with any large-scale cloud allocated according to a maximum/random overlap assumption in the remaining parts of the column. The ECMWF model uses a maximum/random overlap assumption for its single cloud type, while the LMD model combines convective and large-scale clouds into a single cloud type, which it then overlaps randomly.
2. Cloud optical thickness is calculated so as to be as consistent as possible with the assumptions in the respective models' radiation codes. In the Hadley Centre model, the optical thickness is diagnosed from within the radiation code itself, while the values from the other two models are calculated off-line using diagnosed values of condensed water path and effective radius.

3 Comparisons of the cloud radiative effect

ERBE measures the longwave and shortwave fluxes emitted and reflected by the Earth to space ($F_L^{\uparrow}$ and $F_S^{\uparrow}$ respectively). By selective sampling, estimates are also made of their clear-sky components, $F_{Lc}^{\uparrow}$ and $F_{Sc}^{\uparrow}$. Subtracting the clear-sky flux from the total flux gives a measure of the effect of clouds on the outgoing radiation as seen from space. Reversing the sign, so as to give the effect on fluxes into the climate system rather than to space, gives the cloud radiative effect (C) (often referred to as cloud radiative forcing (Harrison et al. 1990)).

$$C_L = -(F_L^{\uparrow} - F_{Lc}^{\uparrow}) = F_{Lc}^{\uparrow} - F_L^{\uparrow}$$

$$C_S = -(F_S^{\uparrow} - F_{Sc}^{\uparrow}) = F_{Sc}^{\uparrow} - F_S^{\uparrow}$$

This quantity gives a measure of the potential sensitivity of the longwave and shortwave net downward fluxes at the top-of-the-atmosphere to changes in clouds. The diagnostic depends not only on the characteristics of the cloud itself but also on the radiation absorbed and scattered by the surrounding environment. For instance, a highly reflective cloud over a dark ocean will have a larger cloud radiative effect than the same cloud over highly reflective ice. In this way, areas where the top-of-atmosphere longwave and shortwave radiation are sensitive to changes in cloud are highlighted, while little weight is given to those where cloud changes are likely to have little effect on them.

Figure 1 shows the monthly mean shortwave cloud radiative effect for July 1988 from ERBE and from the three models. The four boxed regions denote areas of particular interest which will be examined in more detail, and are referred to here as the mid-latitude north Pacific region, the Californian stratocumulus region, the Hawaii trade-cumulus region and the tropical warm pool region.

The effect of cloud in the shortwave is generally to reflect more sunlight back to space than the surface, giving a net cooling effect. ERBE shows maxima in the magnitude of the shortwave cloud radiative effect ($|C_S|$) over the northern mid-latitude oceans, in the subtropical stratocumulus regions, and in regions of tropical deep convection over India and the Bay of Bengal, the tropical west Pacific, along the Eastern Pacific in Atlantic inter-tropical and southern-Pacific convergence zones and in the southern Pacific convergence zone. Local minima occur in $|C_S|$ mainly in the subtropical subsidence regions, for instance in Northern Hemisphere trade-cumulus regions, and over the Sahara desert and the west coast of the United States.

Note that strong contrasts are seen between the values of $|C_S|$ in adjacent regions, for example, between the Hawaii trade-cumulus region and the stratocumulus region to the east. This contrast is due to the prevalence of different cloud types which tend to occur in regions with different boundary layer structures (e.g. trade cumulus in convectively mixed boundary layers over warm SSTs, or stratocumulus in well-mixed boundary layers over cooler SSTs.) As SSTs increase in climate change experiments, the relative frequency of occurrence of these different boundary layer types could change. The strong contrast between the radiative effect of the clouds in these different boundary layer regimes could then lead to a cloud feedback. If these contrasts are poorly reproduced by models in present-day simulations, it is unlikely that those models will show much skill in reproducing such 'cloud regime' type feedbacks.

Comparing Fig. 1(a and b–d) shows that, whilst all three climate models reproduce the broad distribution of $|C_S|$ they all have significant (and different) errors of detail. In the northern Pacific region, $|C_S|$ is significantly

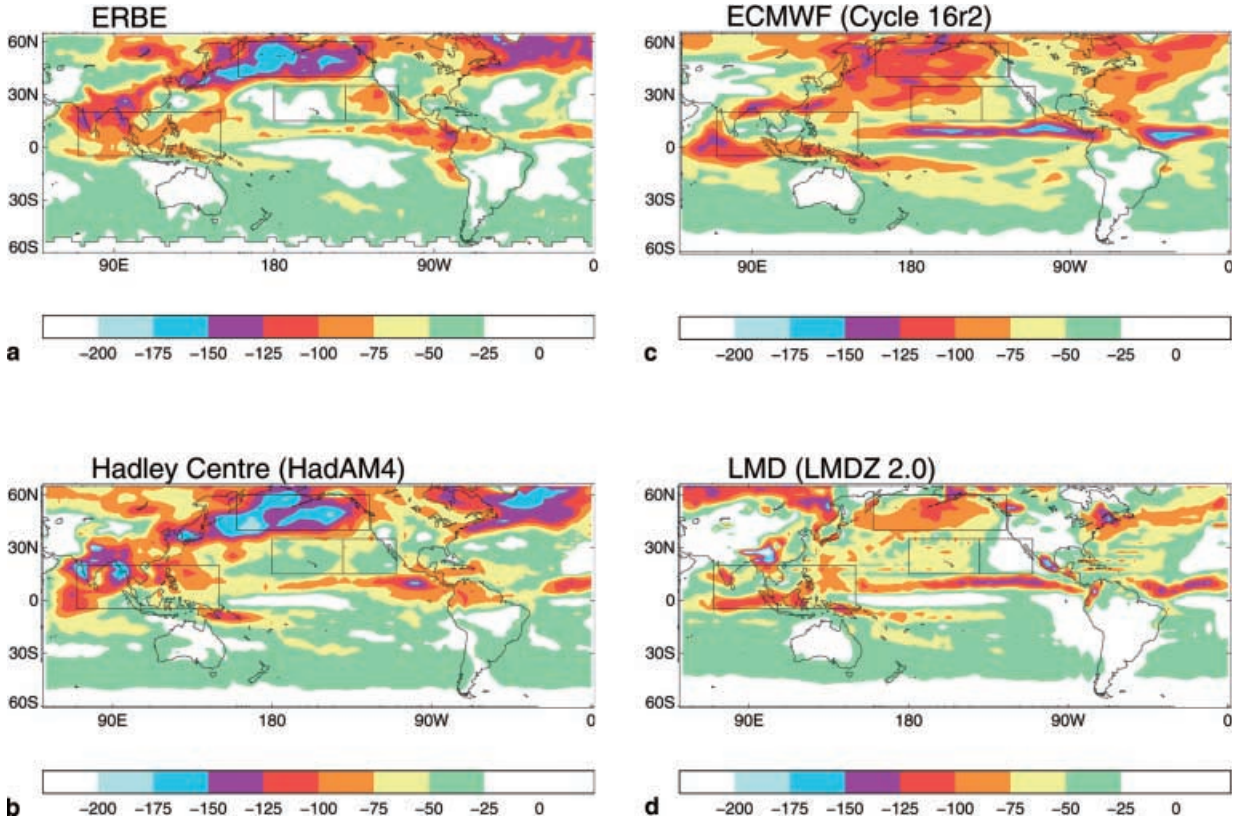

Fig. 1a–d The monthly averaged shortwave cloud radiative effect for July 1988, observed and modelled: **a** ERBE, **b** Hadley Centre, **c** ECMWF and **d** LMD

underestimated by the ECMWF and LMD models, while all three models underestimate $|C_S|$ in the Californian stratocumulus region. In fact, each of the models has a local minimum in this region where the observations show a local maximum. To the west, in the Hawaii trade-cumulus region, the models all tend to overestimate $|C_S|$ to some extent, although the Hadley Centre model does seem to be able to reproduce the observed local minimum, unlike the other two models. In the tropical warm pool region, the ECMWF and LMD models show a slight underestimate in $|C_S|$ particularly over India and the Bay of Bengal.

In all three models these errors cause the contrast in $|C_S|$ between the three regions in the Northern Hemisphere Pacific to be underestimated. The ECMWF and LMD models underestimate the contrast between the mid-latitude northern Pacific region and the Hawaii trade cumulus region, while the contrast between the Hawaii and Californian stratocumulus regions is the reverse of that observed, with brighter clouds to the west than to the east. The Hadley Centre model slightly underestimates the north Pacific/Hawaii contrast and fails to capture the contrast between the stratocumulus and trade-cumulus regions, having similar values of $|C_S|$ in each area.

The models' difficulties in representing the contrasts between the California and Hawaii regions might be due to specific problems in the models' cloud schemes, their boundary layer schemes, or in the ability of the models to reproduce the large-scale dynamical features of the atmosphere, such as the strength of the Hadley circulation, which are dependent on processes such as convection acting in other regions.

Figure 2 shows the monthly mean longwave cloud radiative effect for July 1988 from ERBE and from the three models. In the longwave, clouds generally warm the planet by replacing thermal radiation emitted by the surface with radiation emitted at a lower temperature. The effect is strongest in the tropics where surface temperatures are higher and the contrast between surface and cloud top temperature is largest.

ERBE (Fig. 2a) shows maxima in the magnitude of the longwave cloud radiative effect ($|C_L|$) in tropical deep convective areas that correspond closely with maxima in $|C_S|$ (see Fig. 1a). A region of high values can be seen to the east of Japan which extends across the Pacific and is clearly associated with the summertime storm track. Note that the large values of $|C_L|$ lie in the southern half of the boxed region, while high values of $|C_S|$ are seen throughout the region (see Fig. 1a). This suggests that high values of $|C_S|$ seen in this region may be due to clouds with tops at higher levels to the south than to the north. A band of intermediate values is also seen across the Southern Ocean. Minima can be seen over much

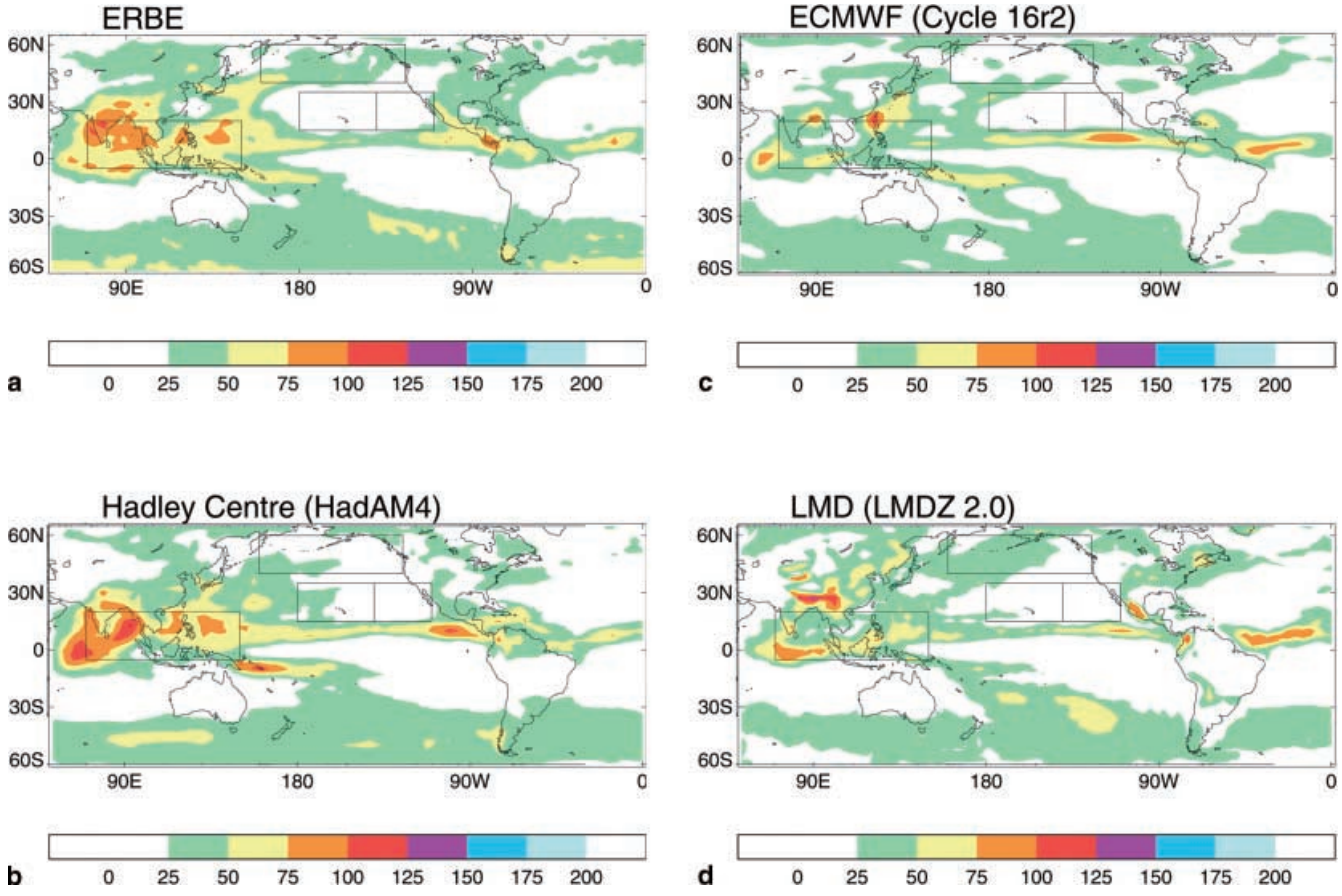

Fig. 2a–d The monthly averaged longwave cloud radiative effect for July 1988, observed and modelled: **a** ERBE, **b** Hadley Centre, **c** ECMWF and **d** LMD

of the subtropics, where descending air minimises the occurrence of clouds with high tops.

Comparing Fig. 2(a and b–d) shows again that the main features of the distribution are reproduced in varying degrees by the three climate models. The Hadley Centre model represents the maximum in the north Pacific region reasonably well, although the area with $|C_L|$ greater than 25 W/m^2 is too small, leading to an underestimate over the region. The ECMWF model has a similar problem, while the LMD model does the best job at reproducing this feature. The small values of $|C_L|$ in the Californian stratocumulus region are reproduced by all of the models, although each also shows a slight tendency to overestimate $|C_L|$ in the Hawaii trade-cumulus region with higher values encroaching from the west.

In the tropical warm pool region the ECMWF and LMD models tend to underestimate $|C_L|$. Note that these underestimates are larger than the underestimates seen in $|C_S|$ in percentage terms. If a model reproduces the correct types of clouds in a region and also treats cloud consistently in the longwave and shortwave, a percentage underestimate in the total amount of cloud should lead to equal percentage underestimates in the longwave and shortwave components of the cloud radiative effect. The fact that this is not seen in either of the models suggests the problem is more fundamental than a general underestimate in the amount of cloud, for example that there is a problem with the distribution of high versus low clouds, or that the treatment of cloud radiative properties in the shortwave versus the longwave is inconsistent. Evidence is presented in Sect. 4 that suggests the former possibility to be the case.

Overall, regional contrasts in the cloud radiative effect in the shortwave are less well handled by the models than the equivalent contrasts in the longwave. It may be relevant that the longwave cloud radiative effect is less sensitive to variations in cloud water path than the shortwave (as infra-red cloud radiative properties saturate more rapidly with increasing water path) and is determined more by the cloud top temperature/height. The success of the models in representing the contrasts in the longwave may simply be because it is easier for models to simulate cloud top height to within a certain fractional accuracy than cloud water path. Additionally, the difficulty in representing the wide variety of clouds in different boundary layer types will have more of an impact on the shortwave cloud radiative effect, as low clouds contribute more to this than to its longwave counterpart.

These comparisons with ERBE data have characterised the differences between the modelled and observed

distributions of the cloud radiative effect, and have shown problems in various areas, some of which are shared between the shortwave and longwave components, and some which affect one but not the other. Using ERBE data alone, little more can be done to investigate these problems. It is also possible that in those areas where the models are in agreement with ERBE data, compensating errors are conspiring to give agreement for the wrong reasons. In the following section, a combination of ISCCP data and ERBE data is used to isolate the contributions of different cloud types to the errors in the simulations of cloud radiative effect in the three models.

4 Comparisons with ISCCP and ERBE data

4.1 Comparisons in the mid-latitude north Pacific region

Figure 3a shows, for the mid-latitude north Pacific region, a histogram of the frequency of occurrence of cloudy pixels for the 35 ISCCP C1 cloud types, organised by cloud optical thickness and cloud top pressure.

The histogram shows that the cloud type most commonly observed by the ISCCP in this region has an optical thickness in the mid range, with a cloud top retrieved to be at about 750 hPa. A range of cloud types is seen, with tops throughout the troposphere. Frontal clouds extending from the boundary layer to the upper troposphere are common in this region, and will have larger cloud water paths than shallower clouds with lower tops. This may explain the tendency for the clouds in this region to show increasing cloud optical thickness with higher tops.

Figure 3b shows the values of the monthly mean longwave and shortwave cloud effects for the same region, as well as a breakdown of these into contributions from high, mid-level and low top clouds. The quantities presented and their methods of calculation will be described in turn.

C_L and C_S, plotted just beneath the abcissa, are the regionally averaged values of the monthly mean longwave and shortwave cloud radiative effects from ERBE.

nL, nM and nH represent the regionally averaged percentage of occasions in the month when low, mid-level and high-top clouds respectively make the largest contribution to the ISCCP daily mean. To calculate these values, daily mean cloud fractions representing the amount of low top (cloud top pressure $P_c > 680\,hPa$), mid-level top ($680\,hPa >= P_c > 440\,hPa$) and high top ($440\,hPa >= P_c$) cloud seen by the ISCCP from space were diagnosed for each gridpoint in the region, for each day in the month. For a single gridpoint on a particular day, high, mid-level or low top cloud is said to dominate if the amount of cloud of that type is the greatest of the three; this situation may also be described as a low, mid-level or high top cloud dominant event. For each gridpoint, the percentage of occasions during the month for which each cloud type dominated was calculated, and then an average was taken over the whole region to yield nL, nM and nH. Very occasionally there was no cloud observed at all on a particular day, so the three values shown usually add up to slightly less than 100%.

The values plotted in Fig. 3b show that in the mid-latitude north Pacific region, nL is the largest of the three values, which indicates that low top cloud dominant events are the most common in this area. Mid-level clouds dominate about a third of the time (see nM), with the remaining sixth of occasions being dominated by high top clouds (nH).

C_SL represents the contribution to C_S from those occasions when when low-top clouds dominate. This is calculated by averaging the daily mean shortwave cloud radiative effect over all points and days, multiplying each value by a weighting factor (unity when low top clouds dominate, zero otherwise). C_SM and C_SH are the equivalent contributions to C_S from mid-level and high top dominant cloud events.

Figure 3b shows that in the mid-latitude north Pacific region, C_SL is the biggest of the three, which means that the low top-dominant events contribute more to C_S than the mid-level or high top-dominant events. This is not surprising given that nL is greater than nM or nH (i.e. the low-top-dominant events are most common), but it is interesting to note that although the low top clouds (nL) are dominant on about half of the occasions, C_SL makes up less than half of the total value of C_S. (Note that $-nL$, $-nM$, and $-nH$ are also plotted for easier comparison with the shortwave values.)

The effect described may be seen more clearly by looking at C_S/nL, C_S/nM and C_S/nH, which are the conditionally averaged equivalents of C_SL, C_SM and C_SH, averaged only over the days and points where the relevant cloud type dominates. C_S/nL is smaller than C_S/nM and C_S/nH showing that low top dominant events have, on average, smaller daily mean values of C_S than the mid and high top dominant events. This is consistent with the lower cloud optical thicknesses associated with the lower cloud tops discussed (see Fig. 3a), and shows that it is the relatively high percentage of low-top-dominant events (nL) in this region that ensures that these events contribute the most to C_S, rather than the brightness of the low clouds themselves.

The conditionally averaged values of the low, mid-level and high top longwave cloud radiative effect C_L/nL, C_L/nM and C_L/nH show that, as is the case with their shortwave equivalents, the higher the cloud tops, the larger the magnitude of the associated cloud radiative effect. The effect is stronger in the longwave than the shortwave however, and almost completely compensates for the larger frequency of occurrence of low-top-dominant events to give a roughly equivalent contribution to

►

Fig. 3a–h July 1988 monthly averaged ISCCP-like cloud distribution (in percent) in the mid-latitude north Pacific region160°–235°E, 40°–60°N: **a** ISCCP, **c** Hadley Centre, **e** ECMWF and **g** LMD, and a breakdown of the cloud radiative effect in the region according to cloud top pressure: **b** ERBE and ISCCP, **d** Hadley Centre, **f** ECMWF and **h** LMD

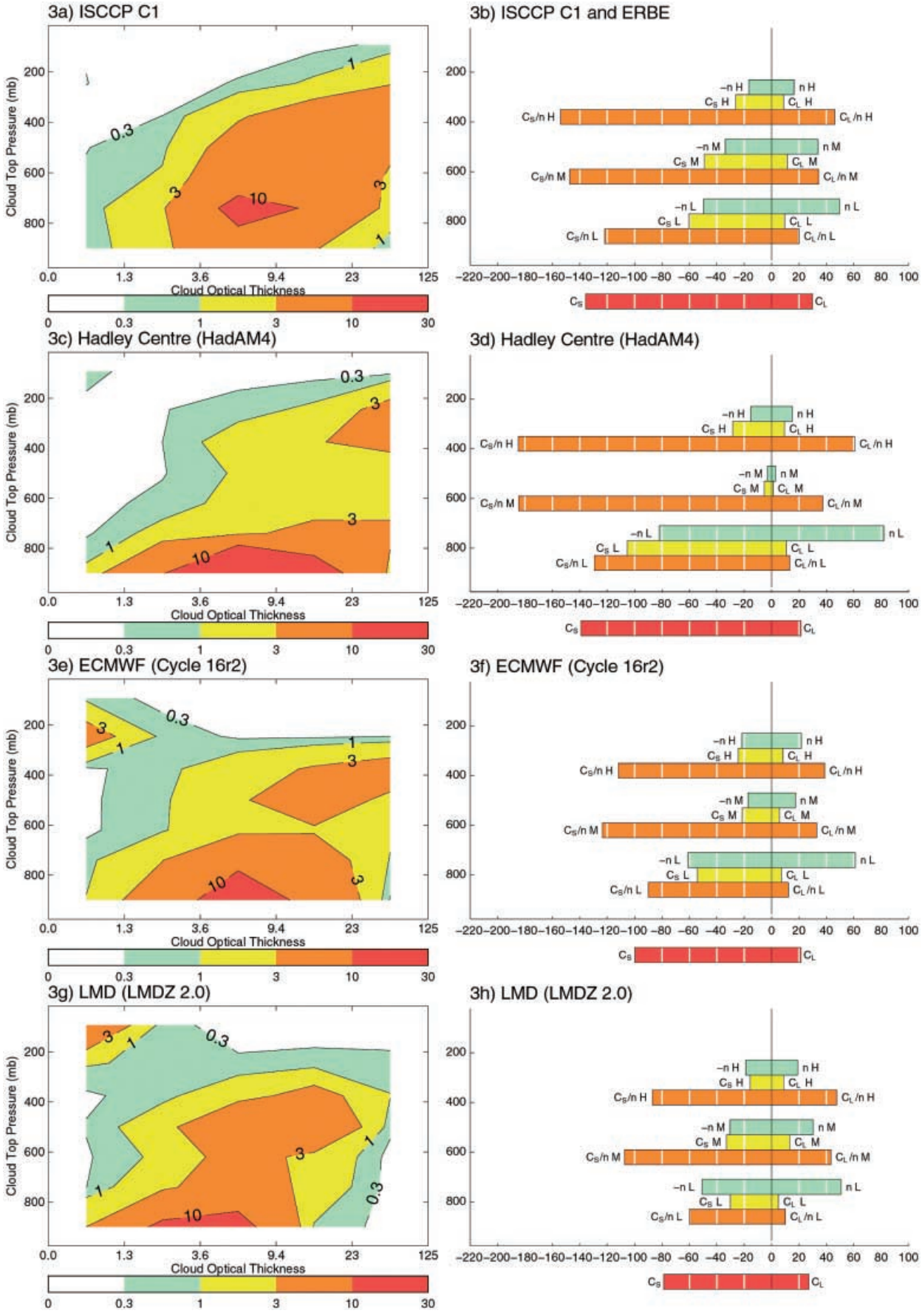
3a) ISCCP C1
3b) ISCCP C1 and ERBE
3c) Hadley Centre (HadAM4)
3d) Hadley Centre (HadAM4)
3e) ECMWF (Cycle 16r2)
3f) ECMWF (Cycle 16r2)
3g) LMD (LMDZ 2.0)
3h) LMD (LMDZ 2.0)
Cloud Top Pressure (mb)
Cloud Optical Thickness
0.0 1.3 3.6 9.4 23 125
0 0.3 1 3 10 30
200 400 600 800
−n H
n H
C_S H
C_L H
C_S/n H
C_L/n H
−n M
n M
C_S M
C_L M
C_S/n M
C_L/n M
−n L
n L
C_S L
C_L L
C_S/n L
C_L/n L
−220 −200 −180 −160 −140 −120 −100 −80 −60 −40 −20 0 20 40 60 80 100
C_S
C_L

the longwave cloud radiative effect from each of the low, mid-level and high top dominant events (see C_LL, C_LM and C_LH).

Given that large values of the longwave cloud radiative effect are usually associated with clouds with high tops, it is perhaps surprising to find that the low top dominant events contribute as much to the monthly mean longwave cloud radiative effect here as do high top dominant events; clearly the relatively small values of C_L associated with individual low cloud events should not be overlooked, as they occur sufficiently frequently to make a significant contribution to the total.

Figure 3c shows an equivalent histogram from the Hadley Centre model, which shows the model to reproduce both the observed optically thicker clouds with high tops and the intermediate optical thickness clouds with tops in the boundary layer, but to have less intermediate optical thickness cloud with tops at mid and high levels than observed, and more cloud with low tops and high optical thicknesses. This is reflected in the values plotted in Fig. 3d, which show a serious underestimate in nM, the frequency of mid-level dominant events, accompanied by a significant overestimate in nL, the frequency of low cloud dominant events. This leads to an underestimate in C_SM, the contribution to C_S from the mid level top dominant events. This is however compensated for by a larger-than-observed contribution from the low cloud dominant events (C_SL), giving a total value of C_S in rough agreement with the observed value from ERBE. A tendency to overestimate the conditionally averaged values C_S/nL, C_S/nM and C_S/nH by about 20% is noted, although these errors are relatively small compared with the problems with distribution of the dominant cloud type events nL, nM and nH.

In the longwave, the contribution to C_L from the mid-level cloud (C_LM) also suffers, but the higher frequency of occurrence of low level top dominant events fails to compensate via C_LL as well as it does in the shortwave. This is because the low top conditional average C_L/nL is only a third of that for mid-level-top events (C_L/nM), while the shortwave equivalents are much more comparable; this makes it harder for low clouds to compensate for a lack of mid-level clouds in the longwave than in the shortwave.

The situation described illustrates the benefit of using a combination of datasets when assessing model cloud simulations; compensating errors may be discovered that might otherwise go undetected. In view of this, a model's agreement with the observed monthly mean shortwave cloud radiative effect while errors remain in the longwave should be interpreted carefully, as it may well stem from such a compensation of errors.

Figures 3e and f show the equivalent histogram and plot for the ECMWF model. The similarity between the distributions of cloud in the ECMWF and Hadley Centre models is striking, with a similar underestimate in the amount of intermediate optical thickness cloud with tops at mid and high levels. Less optically thick cloud with low tops is seen however, and many of the upper level cloud tops are slightly lower than those 'retrieved' from the Hadley Centre model. The latter difference is a consequence of the cloud retrieval-like method used to diagnose cloud top pressure from the models. Frontal clouds in the ECMWF model have large water paths (and hence large cloud optical thicknesses) in the liquid parts of the cloud at lower levels, while having small ice water paths at upper levels. As a consequence of this, the ISCCP-like model processing, which diagnoses the cloud top at the level of an equivalent emitting temperature to that observed, can diagnose upper level clouds as having tops as much as 200 hPa below the level at which they actually reside in the model (Jakob personal communication). Were a similar situation to arise in the real world, ISCCP would be likely to underestimate the cloud top height to a similar degree. In practice this happens only infrequently around the edges of cloud systems (Rossow personal communication).

The values plotted in Fig. 3f show a similar but smaller underestimate in nM, the frequency of mid-level top dominant events, to that seen in the Hadley Centre model (although the size of this underestimate may have been reduced by the effect discussed). This leads once again to an underestimate in the contribution to the shortwave cloud radiative effect from mid-level cloud dominant events (C_SM). In this case, however, the error in the shortwave is not compensated for by an over-estimated contribution from the low top dominant events, (see C_SL), leading to an underestimate in the total value of C_S. In the case of the longwave, the conditional values C_L/nL, C_L/nM and C_L/nH are all slightly underestimated; the problem is made slightly worse in the contribution to the total from C_LM by the underestimate in nM, but is offset slightly in C_LL and C_LH by slight overestimates in the values of nL and nH.

It seems that the cloud simulations of the two models share a basic problem with regard to the mid-level clouds, which reduces both the longwave and shortwave cloud radiative effect in these areas; however in the Hadley Centre model a second problem is present with the low cloud which serves to compensate for the first problem in the shortwave, but fails to do the same in the longwave.

Figure 3g and h show the equivalent histogram and plot for the LMD model. The simulation of mid-level top and intermediate optical thickness cloud is in better agreement with that observed than the other two models, although the optically thick clouds with high tops are under-represented. Consequently, the value of nM for the LMD model in this region is the closest of the three models to the that observed. The mid-level top dominant contribution to the longwave cloud radiative effect C_LM is in good agreement with the observed value, helping to keep the errors in the total longwave cloud radiative effect relatively small. In the shortwave however, the low and mid-top dominant contributions C_SL and C_SM fall short of the observed values. This cannot be explained by errors in the number of low and mid-top-dominant events nL and nM, but is due to under-

estimates in the magnitude of C_S/nL and C_S/nM. These problems are consistent with the underestimate in the amount of low and mid-level top cloud with high optical thicknesses seen in Fig. 3g.

In all, the simulation of the LMD model in this region has a quite different character to those of the other two models. The simulation of the vertical distribution of the cloud agrees well with that observed, which no doubt contributes to the agreement between the simulated and observed values of the monthly mean longwave cloud radiative effect in the region. Although it shares the ECMWF model's tendency to underestimate the shortwave cloud radiative effect in the region, this is due to problems representing the optically thicker clouds, rather than a lack of mid-level clouds visible from above as with the former model.

Considering the possible differences between the models that could account for the varying skill of representing the amounts of cloud with mid-level tops visible from above, two possibilities present themselves:

The first is the use of a random cloud overlap assumption in the LMD model, in contrast to the mixed (also known as maximum-random) cloud overlap assumption used in the other two models. In the former case, clouds of similar extent in consecutive vertical levels will be distributed so that some cloud in each level is visible from above (assuming the cloud extent in each layer is less than 100%.) In the latter case, consecutive cloud levels are maximally overlapped, so a cloud will completely obscure another cloud of equivalent extent in the level immediately below it. In this way, one can see how the different overlap assumptions could partially explain the differences seen in the simulations.

The second possibility relates to the convection schemes used in the three models. The LMD model uses a simple moist adjustment scheme, which relaxes the model's temperatures and humidities towards a smoothly varying standard profile. This approach is likely to give a smoother vertical profile of temperature and humidity (and hence roughly equivalent amounts of cloud at all levels) than that generated by one of the more detailed mass flux schemes used in the other two models, which may detrain in the upper troposphere, generating more cloud there than in the mid troposphere. Many of the more detailed convection schemes in use today use parameters based on data gathered in the deep tropics, and may not be well optimised for performance in the mid-latitudes.

4.2 Comparisons in the Californian stratocumulus region

Figure 4a shows a histogram depicting the frequency of occurrence of cloudy pixels observed by the ISCCP in the Californian stratocumulus region, as a function of cloud optical thickness and cloud top pressure.

The most commonly observed cloud type in this region has a retrieved cloud optical thickness of around 10, with a cloud top pressure of about 800 hPa. Figure 4b shows that, unsurprisingly, low-top-dominant cloud events are the most common (see nL, nM, nH) and most of the shortwave and longwave cloud radiative effect in this area is attributable to these (see C_S, C_SL, C_L and C_LL).

All three models (Fig. 4c, e, g) share a tendency to underestimate the total amount of cloud in this region. They also have lower cloud optical thicknesses on average than those retrieved by the ISCCP. These problems lead to varying underestimates in shortwave and longwave cloud radiative effect associated with low cloud events, which, as with the observations, contribute most to the total values of cloud radiative effect.

Note also that all of the models show typical boundary layer cloud tops to be lower than those retrieved by the ISCCP. It is either the case that all of the models share a common problem with underestimated boundary layer depths, or that the ISCCP retrieval overestimates the height of the boundary layer cloud tops (a possibility if in reality a thin layer of cirrus is present high above the boundary layer clouds). In-situ measurements collected during FIRE mostly had boundary layer tops in the region of 900 hPa (Field personal communication), suggesting that some problem with the ISCCP retrieval is a likely possibility.

4.3 Comparisons in the Hawaii trade-cumulus region

Figure 5a shows a histogram depicting the cloud distribution in the Hawaii trade-cumulus region. The most commonly observed cloud type in this region has a retrieved cloud optical thickness in the mid range, with cloud tops in the lower troposphere. Figure 5b shows that, as in the Californian stratocumulus region, low top dominant cloud events are the most common (see nL, nM, nH) and the majority of the shortwave and longwave cloud radiative effect in this area comes from low clouds (see C_S, C_SL, C_L and C_LL).

Figure 5c shows the Hadley Centre model to have less low top cloud than observed, but more high top cloud. The low top cloud forms two populations, one with an optical thickness in reasonable agreement with the observed values, but another which tends to be optically thicker than the ISCCP retrievals. There is more high top cloud in this region than observed, with a range of cloud optical thicknesses. Figure 5d shows there to be fewer low top dominant events than observed (see nL), but more high top dominant events (nH). The contribution to the shortwave cloud radiative effect from the low top dominant events (C_SL) is in good agreement with the observations; the overestimate in the total is mainly due to the excess of high top dominant events (see nH and C_SH). This problem also contributes to the model's overestimate in C_L in the region (see C_LH) and could be related to mid-latitude weather systems encroaching into the region more frequently than in reality.

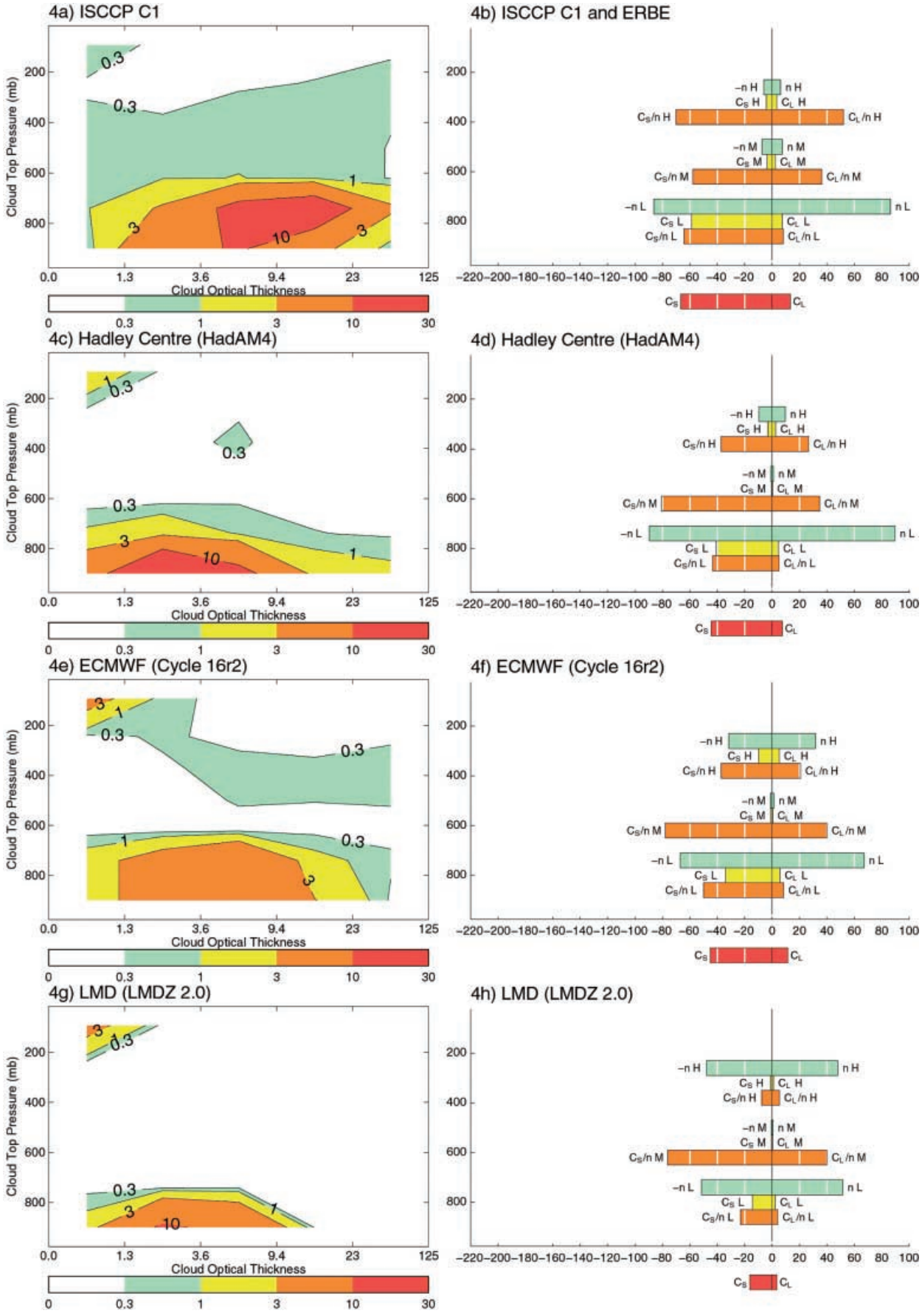
4a) ISCCP C1
4b) ISCCP C1 and ERBE
4c) Hadley Centre (HadAM4)
4d) Hadley Centre (HadAM4)
4e) ECMWF (Cycle 16r2)
4f) ECMWF (Cycle 16r2)
4g) LMD (LMDZ 2.0)
4h) LMD (LMDZ 2.0)
Cloud Top Pressure (mb)
Cloud Optical Thickness
0.0 1.3 3.6 9.4 23 125
0 0.3 1 3 10 30
200 400 600 800
0.3
1
3
10
−n H
n H
Cs H
CL H
Cs/n H
CL/n H
−n M
n M
Cs M
CL M
Cs/n M
CL/n M
−n L
n L
Cs L
CL L
Cs/n L
CL/n L
−220 −200 −180 −160 −140 −120 −100 −80 −60 −40 −20 0 20 40 60 80 100
Cs
CL

◄

Fig. 4a–h July 1988 monthly averaged ISCCP-like cloud distribution in the Californian stratocumulus region 220–250°E, 15–35°N: **a** ISCCP, **c** Hadley Centre, **e** ECMWF and **g** LMD, and a breakdown of the cloud radiative effect in the region according to cloud top pressure: **b** ERBE and ISCCP, **d** Hadley Centre, **f** ECMWF and **h** LMD

Figures 5e and f show the ECMWF model to have a similar problem to the Hadley Centre model, in that more high-top-dominant events are seen than observed, contributing to an overestimate in the longwave and shortwave components of the cloud radiative effect in this area (see nH, C_S, C_SH, C_L, C_LH.) However, the low level clouds are on average optically thicker than the equivalent retrieved values (Fig. 5e), and so cause an overestimate in the low top dominant contribution to the shortwave cloud radiative effect (see C_S/nL and C_SL) so that the over-estimates from the low and high components contribute equivalent amounts to the overestimate of the magnitude of C_S in this region.

Figure 5g shows the LMD model to have more low top cloud than is observed in the region, as well as a larger mean cloud optical thickness than retrieved by ISCCP, leading to an overestimate in the magnitude of C_S, mostly from low top dominant cloud events (see C_S/nL and C_SL in Fig. 5h).

4.4 Comparisons in the tropical warm pool region

Figure 6a shows the observed cloud distribution in the tropical warm pool region. The most commonly retrieved cloud tops in this region are in the upper troposphere, with optical thicknesses covering a range of values from optically thin to thick. Note that there is a tendency for pixels with cloud top pressures in the upper troposphere and column optical thicknesses around 3 to have retrieved cloud tops slightly lower than those with higher optical thicknesses. The fact that some pixels are seen with cloud top pressures in the low and mid-troposphere and with similar optical thicknesses suggests that this may be due to a multi-layer cloud effect, where a layer of optically thin cirrus lies above a layer of low cloud with an intermediate optical thickness around 3, and is interpreted by ISCCP as a single cloud with an optical thickness of around 3 with a cloud top pressure in between those of the two layers. Figure 6b shows that high top dominant cloud events are the most common in this region (see nH) and that these events contribute the majority of the total longwave and shortwave cloud radiative effects (see C_S, C_SH, C_L and C_LH).

The Hadley Centre model (Fig. 6c) represents the cloud in this region relatively well, showing a range of cloud optical thicknesses in the upper troposphere, although more optically thin cloud is seen than is retrieved by the ISCCP, and significant variations in 'retrieved' cloud top pressure in the upper troposphere are not seen. A little boundary-layer cloud is also seen with optical thickness close to that retrieved by the ISCCP, although fewer clouds with mid-level tops are seen. Figure 6d shows that the high-top-dominant events are by far the largest contributors to the longwave and shortwave cloud radiative effect in the region, as is the case in the observations (see C_S, C_SH, C_L and C_LH).

The ECMWF model (Fig. 6e) reproduces the observed amount of optically thin and optically thick cloud with high tops in the region, but has less cloud of intermediate optical thickness, and more optically thick boundary layer cloud than is retrieved by the ISCCP. Figure 6f shows that while the number of high top dominant events nH is slightly underestimated, the underestimate in the contribution from this cloud type to the longwave and shortwave components of the cloud radiative effect C_SH and C_LH is mainly due to an underestimate in the conditional averages C_S/nH and C_L/nH. The excessively optically thick clouds in the boundary layer partially offset this problem by boosting the magnitude of the contribution from low top dominant events (see C_S/nL and C_SL) and so reducing the error in C_S. This explains the relative difference in the severity of the underestimates in the magnitudes of C_S and C_L in the region.

The LMD model (Fig. 6g) has a similar problem to the ECMWF model in that it has too little cloud with intermediate cloud optical thicknesses in the upper troposphere, causing an underestimate in the longwave and shortwave components of the cloud radiative effect associated with high top dominant cloud events (see nH, C_SH and C_LH in Fig. 6h). As with the ECMWF model, the impact of this problem on the total value of C_S is partially compensated for by an excessive contribution from low top clouds (see nL, C_S/nL, C_SL and C_S), in this case with intermediate cloud optical thicknesses.

It is interesting to note that compensations between different cloud types that lead to the models having the right cloud radiative effect in a particular region for the wrong reasons seem to be more common in the shortwave than in the longwave. This is probably because there is little contrast between the conditionally averaged cloud radiative effects of typical low, mid-level and high top dominant events in the shortwave, which makes it easier for low clouds to compensate for a lack of mid or high top cloud than is the case in the longwave where the cloud radiative effect of low clouds is small compared with that of high clouds.

5 Relationships between cloud amount and the radiation budget

Slingo (1990) showed that relative increases of 15–20% in the amount of low cloud in a modified version of the NCAR Community Climate Model were able to balance the globally meaned top-of-atmosphere radiative forcing due to doubling present day carbon dioxide concentrations. This sensitivity of the radiation budget to cloud amount depends on the relationships between cloud amount and albedo and between cloud amount and outgoing longwave radiation at the top of the atmosphere.

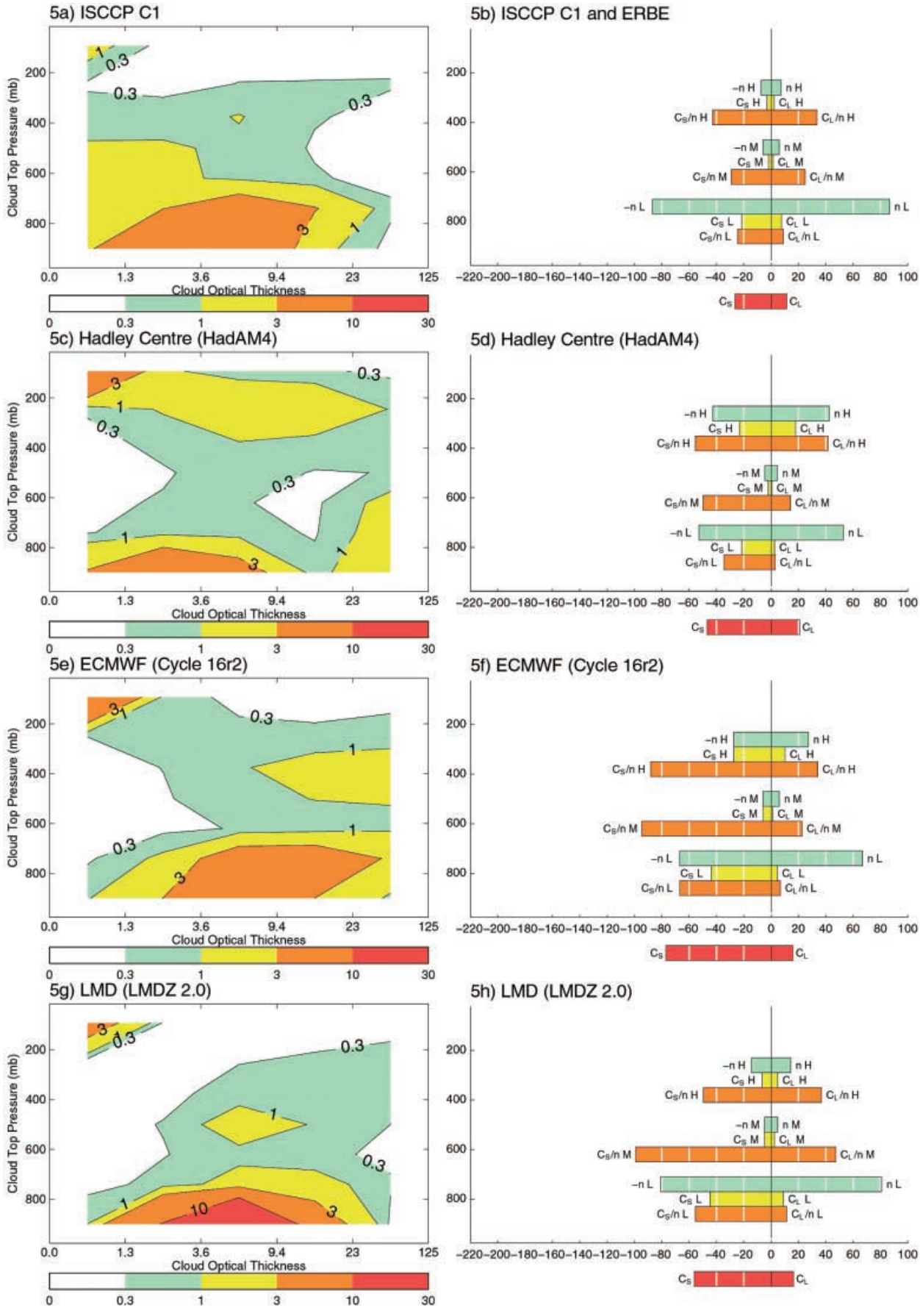
5a) ISCCP C1
5b) ISCCP C1 and ERBE
5c) Hadley Centre (HadAM4)
5d) Hadley Centre (HadAM4)
5e) ECMWF (Cycle 16r2)
5f) ECMWF (Cycle 16r2)
5g) LMD (LMDZ 2.0)
5h) LMD (LMDZ 2.0)
Cloud Top Pressure (mb)
Cloud Optical Thickness
0.0 1.3 3.6 9.4 23 125
0 0.3 1 3 10 30
200 400 600 800
−n H
n H
Cs H
CL H
Cs/n H
CL/n H
−n M
n M
Cs M
CL M
Cs/n M
CL/n M
−n L
n L
Cs L
CL L
Cs/n L
CL/n L
−220 −200 −180 −160 −140 −120 −100 −80 −60 −40 −20 0 20 40 60 80 100
Cs
CL

◄

Fig. 5a–h July 1988 monthly averaged ISCCP-like cloud distribution in the Hawaii trade-cumulus region 180–220°E, 15–35°N: **a** ISCCP, **c** Hadley Centre, **e** ECMWF and **g** LMD, and a breakdown of the cloud radiative effect in the region according to cloud top pressure: **b** ERBE and ISCCP, **d** Hadley Centre, **f** ECMWF and **h** LMD

Figures 7 and 8 depict the observed and modelled relationships between these quantities, diagnosed by creating two-dimensional histograms of daily mean cloud amount and albedo (Fig. 7) and daily mean cloud amount and −OLR (minus one times the outgoing longwave radiation) (Fig. 8). The value at a point on the histogram represents the area of the Earth's ocean surface that is covered with clouds of a similar cloud amount and albedo (or value of −OLR). In each case the histogram is a mean of several daily mean histograms calculated for each day of July 1988.

The observations in Fig. 7a show a weakly non-linear relationship between daily mean albedo and daily mean cloud amount with a gentle slope and small scatter for low cloud amounts and a steeper slope and larger scatter as cloud amounts increase. The presence of this non-linearity suggests that cloud optical thickness increases with cloud amount. Cloud optical thickness continues to rise after cloud amounts reaches a value of one, as can be deduced from the large range of albedos with cloud amounts of this value.

Figure 8a shows the observed relationship between cloud amount and −OLR at the top-of-the-atmosphere. The higher (least negative) values of −OLR at around -150 W/m^2 correspond with significant amounts of infra-red trapping associated with clouds in areas with large values of the longwave cloud radiative effect, while less of a warming effect is seen in areas with smaller cloud amounts and values of −OLR in the region of -300 W/m^2. As with the albedo, the observations show a weakly non-linear relationship between −OLR and cloud amount with a gentle slope and small scatter for low cloud amounts and a steeper slope and larger scatter as cloud amounts increase. Again, the largest radiative effect is associated with cloud amounts close to one, and the range of values in −OLR here is indicative of cloud tops at levels throughout the troposphere.

It is clearly desirable for climate models to be able to reproduce these sorts of observed relationships. Firstly, these relationships are likely to affect the sensitivity of the radiation budget to perturbations in total cloud amount, so any model that fails to capture these relationships is likely to misrepresent cloud feedbacks that involve changes in amount. Secondly, estimates of the effect of aerosols on climate via changes to cloud albedo and lifetime, and of direct radiative forcings such as those from sulfate, dust and soot aerosols can be highly sensitive to errors in the simulation of cloud amount and cloud radiative properties; systematic errors in the relationships described could seriously limit the ability of climate models to represent realistically the climate forcings associated with these processes.

Examination of Fig. 7a and b shows that the Hadley Centre model reproduces the broad character of the observed relationship between cloud amount and cloud albedo, demonstrating that the shortwave cloud radiative properties are not inconsistent with those of the observed clouds. However, fewer points than observed are seen with cloud amounts near one, and a slight underestimate in the fraction of the Earth's surface with cloud amounts between 0.75 and 1 is also evident, suggesting the relative amounts of the different cloud types could be improved.

The ECMWF model (Fig. 7c) shows a steeper, but more linear relationship than observed, with generally higher-than-observed albedos for a given cloud amount, suggesting disagreement between the observed and modelled relationships between cloud amount and cloud properties (e.g. cloud water path, droplet/particle size, etc.) As with the Hadley Centre model, the fraction of the Earth's ocean surface overlaid by cloud amounts above about 0.6 is underestimated.

The LMD model (Fig. 7d) shows a clear separation into two cloud type populations; one has a mean value of cloud fraction around 50% and another has cloud fractions closer to one. The first population lies along the observed curve, but too many points have cloud fractions near 50%, with too few in the region of 20% and 85%. The second population agrees well with the observations, although more points with cloud amounts near one and albedos less than 30% than are observed. The LMD results can be explained bearing in mind a few facts about the cloud parametrisations. Firstly, the cloud fraction is the maximum of the three cloud fractions diagnosed; since the cloud fraction associated with the moist adjustment is one, the final cloud fraction will be one as soon as this scheme is activated (i.e. whenever the atmosphere is unstable and saturated). These clouds appear at the expense of the cloud population around 75%. Secondly, because the skewness of the total water PDF used in the LMD model is zero, the non-convective cloud fraction will be overestimated, especially for small cloud fractions. Finally, the cloud fraction used in the model can be of non-convective origin and exceed 50% only if the atmosphere is over-saturated and the moist adiabatic adjustment not active. This happens infrequently.

Figure 8b shows the Hadley Centre model to have a slightly steeper-than-observed relationship between cloud amount and −OLR with more infra-red trapping than is observed for cloud amounts around 75%. Further investigation of this (not shown) shows that these clouds reside mostly in the warm pool region examined already, and suggests that the discrepancy between modelled and retrieved cloud top pressures for cloud optical thicknesses around 3, discussed in Sect. 4, has some bearing on the problem; i.e. where ISCCP retrieves mid-level cloud tops of optical thickness around 3, there could in fact be low cloud with optical thickness around three with optically thinner cloud high above it. If this were the case, then it would mean that some of the model's upper level clouds are too optically thick, which

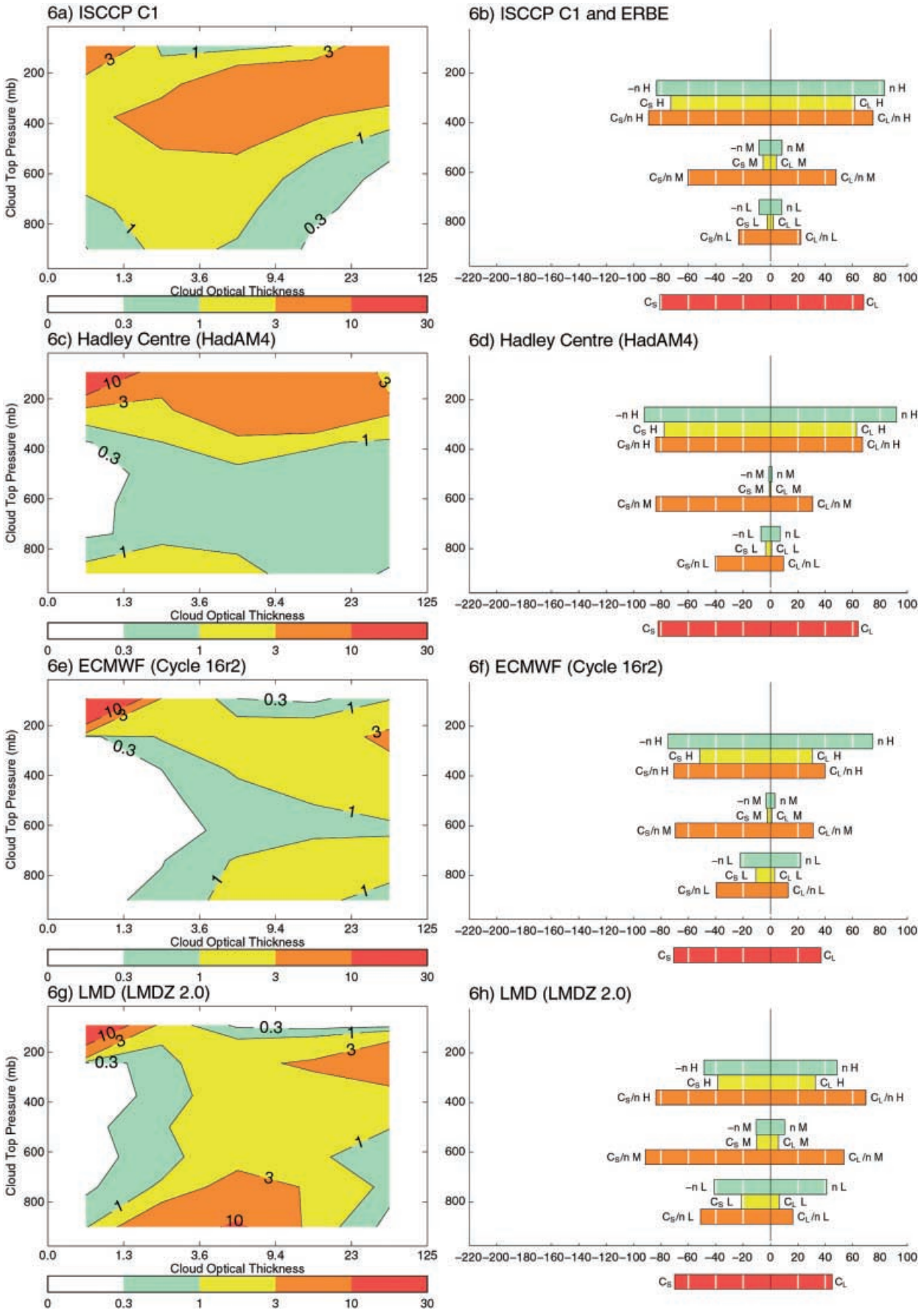
6a) ISCCP C1
6b) ISCCP C1 and ERBE
6c) Hadley Centre (HadAM4)
6d) Hadley Centre (HadAM4)
6e) ECMWF (Cycle 16r2)
6f) ECMWF (Cycle 16r2)
6g) LMD (LMDZ 2.0)
6h) LMD (LMDZ 2.0)
Cloud Top Pressure (mb)
Cloud Optical Thickness
0.0 1.3 3.6 9.4 23 125
0 0.3 1 3 10 30
200 400 600 800
−n H
n H
Cs H
CL H
Cs/n H
CL/n H
−n M
n M
Cs M
CL M
Cs/n M
CL/n M
−n L
n L
Cs L
CL L
Cs/n L
CL/n L
−220 −200 −180 −160 −140 −120 −100 −80 −60 −40 −20 0 20 40 60 80 100
Cs
CL

◄

Fig. 6a–h July 1988 monthly averaged ISCCP-like cloud distribution in the tropical warm pool region 70–150°E, 5°S–20°N: **a** ISCCP, **c** Hadley Centre, **e** ECMWF and **g** LMD, and a breakdown of the cloud radiative effect in the region according to cloud top pressure: **b** ERBE and ISCCP, **d** Hadley Centre, **f** ECMWF and **h** LMD

would be consistent with the results seen in the −OLR histogram. The amount of infra-red trapping associated with the (too few) points with cloud amounts near one also seems to be overestimated. The bimodal nature of the distribution here may be due a lack of mid-level convective cloud tops.

The ECMWF model has similar problems, with larger amounts of infra-red trapping than observed for cloud amounts above 60%. It also shows too much partial cover, with too little full cover.

The LMD model does the best job of capturing the gentle slope of the relationship for cloud amounts up to 75%, but fails to capture the increase in slope for cloud amounts between 75% and one. Like the cloud amount/albedo relationship, the longwave relationship shows a range of values of −OLR for cloud amounts close to one, as is observed. As these clouds are mainly generated by the convection scheme, this range probably reflects the different levels at which convection terminates in the model.

No single model examined successfully reproduces all of the features of the observed relationships between these quantities; consequently there is reason to doubt the abilities of the individual models to represent the radiative impact of variations in cloud amount alone. However, most features of the observed relationships are captured by one model or another, so it should in principle be possible to improve our confidence in the models abilities to represent these simple 'cloud amount' type feedbacks. Further detailed model intercomparisons will help to accelerate this process.

6 Discussion

Uncertainty associated with cloud feedbacks during climate change is a major contributing factor to the wide range in estimates of climate sensitivity due to a doubling of CO_2 (1.5 °C to 4.5 °C e.g. Kattenberg et al. 1996). The cloud feedbacks in climate models need to be

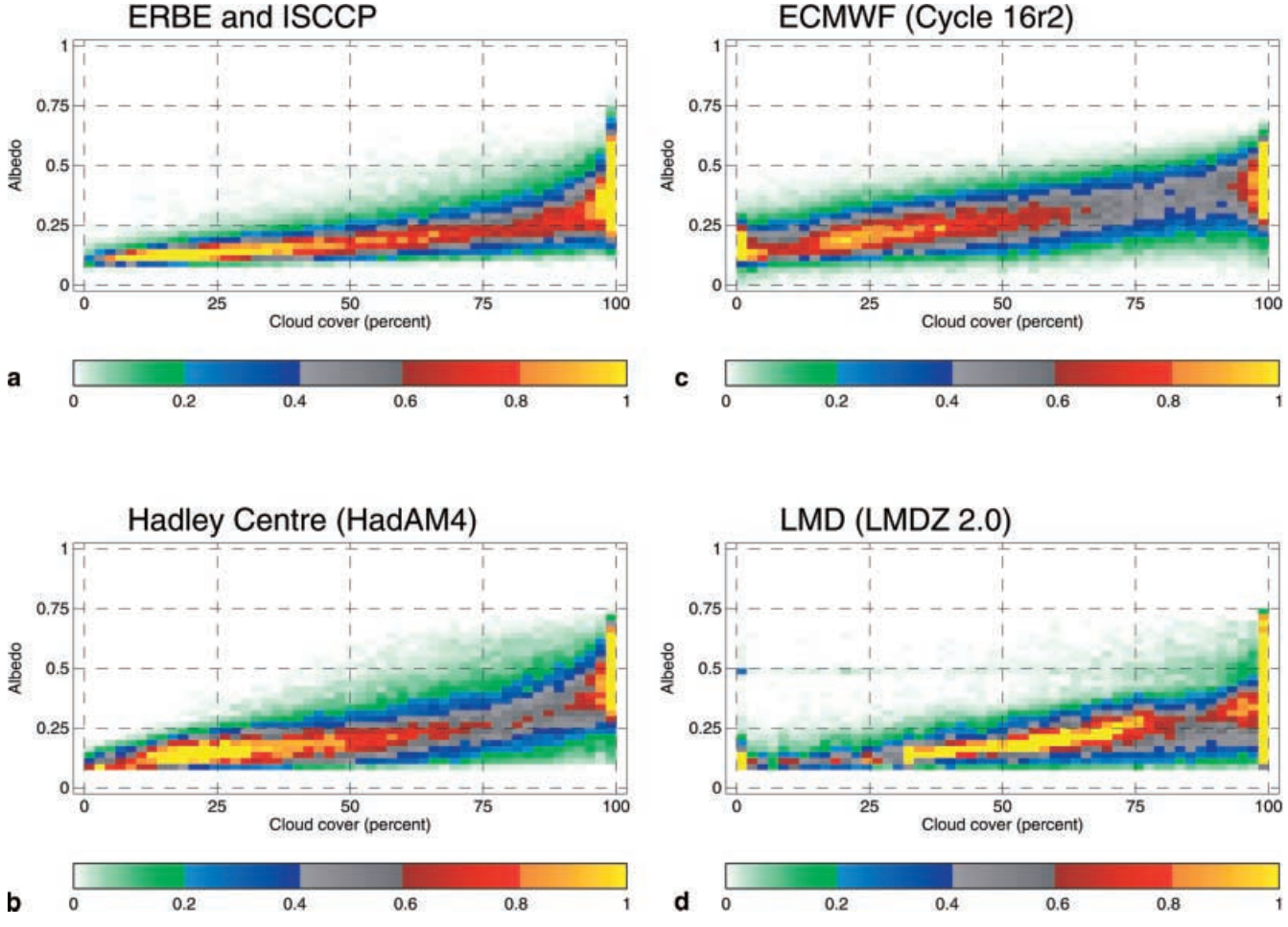

Fig. 7a–d Monthly averaged histograms of daily mean cloud amount and albedo for July 1988: **a** ISCCP and ERBE, **b** Hadley Centre, **c** ECMWF and **d** LMD

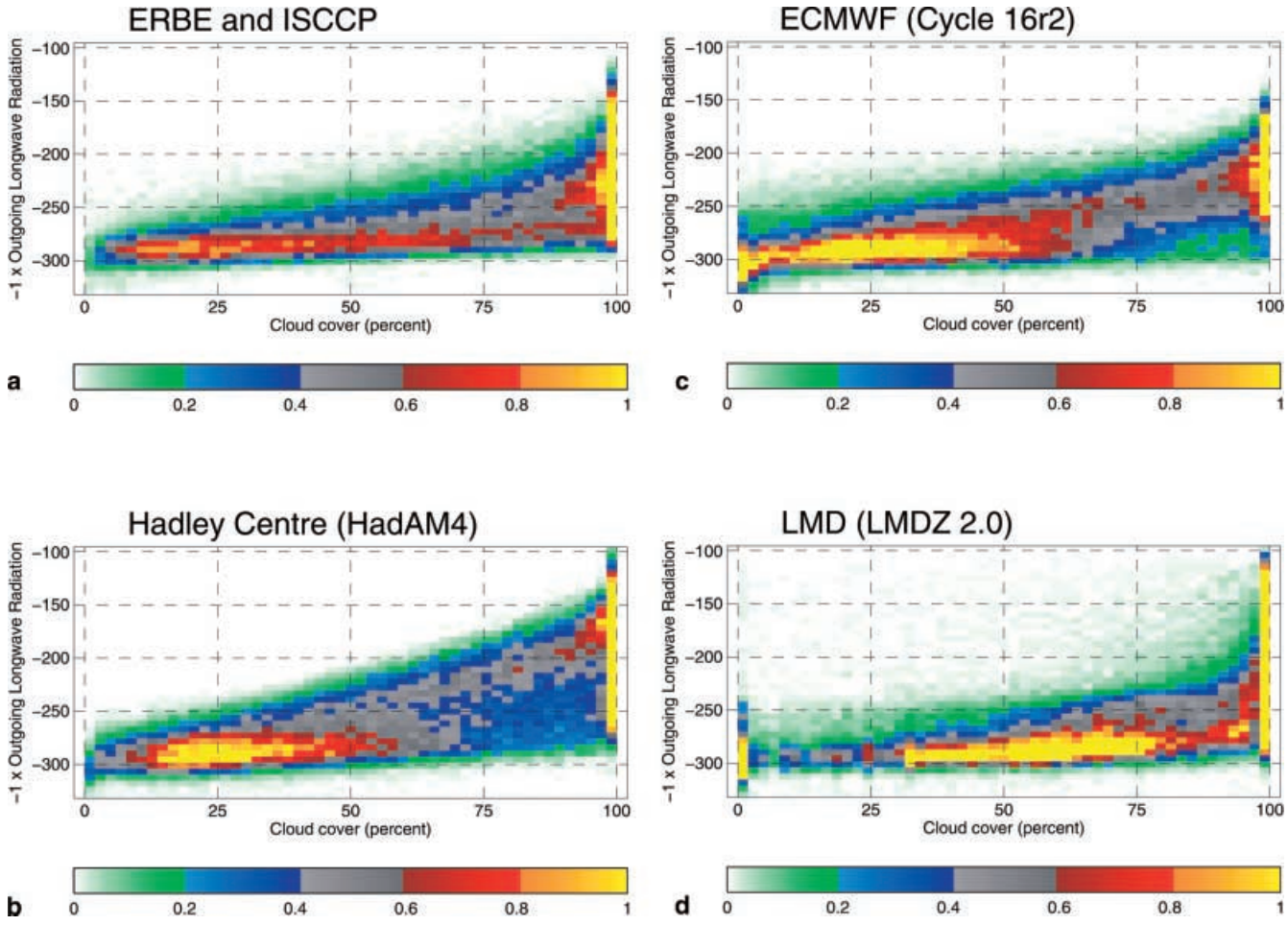

Fig. 8a–d Monthly averaged histograms of daily mean cloud amount and -OLR for July 1988: **a** ISCCP and ERBE, **b** Hadley Centre, **c** ECMWF and **d** LMD

linked to the observed behaviour of clouds, where possible, if this uncertainty is to be reduced. This work presents new techniques designed to assess the realism of climate model cloud simulations taking advantage of multiple datasets providing complementary observations of clouds. These techniques are illustrated by applying ISCCP and ERBE data to the assessment of three climate models.

Analysis of the simulation of monthly mean cloud radiative effect shows errors in various regions, and that the models often fail to capture the local contrasts between adjacent cloud regimes. As the planet warms, it is possible that cloud feedbacks may arise through a transition from one cloud type regime to another in a manner analogous to the transitions between stratocumulus and trade cumulus that take place during local warmings associated with ENSO. Clearly our confidence in current models' abilities to represent these 'cloud regime' type feedbacks will be low if the models are unable to correctly represent the contrasts between these regimes in present day model simulations.

Stratifying the cloud radiative effect into contributions from low, medium and high cloud dominant events has suggested possible reasons for errors seen in the monthly mean cloud radiative effect. It has also highlighted a second class of model problems that are not apparent when validating the monthly mean cloud radiative effect alone, due to the presence of compensating errors.

Examples of the first type, (which are in varying degrees common to all three models considered here) include a tendency to underestimate the magnitude of the shortwave cloud radiative effect in the Californian stratocumulus region, and to overestimate this quantity in the Hawaii trade-cumulus region. The former is a common error in climate models, and is shown here to be mainly due to underestimates in the amount of cloud rather than cloud optical thickness; it is possible that this is due as much to errors in the local large-scale subsidence as to errors in the cloud parametrisations. Additionally, the models have cloud tops in this region which are lower than those retrieved by ISCCP. This could however be caused by problems with the ISCCP retrievals of cloud top pressure, potentially caused by contamination by optically thin upper level clouds. The overestimate in shortwave cloud radiative effect seen in the trade regions is caused by different factors in the

different models: overly optically thick boundary layer clouds in the ECMWF model, excessive amounts of boundary layer cloud in the LMD model and excessive upper level cloud in the Hadley Centre model. Comparisons of the model data with independent observations (e.g. with FIRE and ASTEX data as in Wood and Field 2000) may help to clarify the causes of these problems, although such comparisons are beyond our scope here.

An example of the second type of error is apparent in the mid-latitude north Pacific region where the Hadley Centre and ECMWF models both underestimate the amount of cloud with mid-level tops visible from above. This would be expected to lead to an underestimate in the magnitude of the total shortwave cloud radiative effect; however while this is the case in the ECMWF model, in the Hadley Centre model overestimates the contribution to the shortwave cloud radiative effect from low cloud, giving a total in agreement with that observed.

Another example is present in the tropical warm pool region, where the LMD and ECMWF models partly compensate for an underestimate in the magnitude of the shortwave cloud radiative effect associated with high cloud by contributing more than observed from low clouds. In each case this compensation fails to offset an associated underestimate in the total longwave cloud radiative effect; from this it should be noted that a model that simulates the shortwave cloud radiative effect well in a particular area while underestimating the magnitude of the longwave cloud radiative effect is likely to be achieving the former through a compensation of errors.

It is important to remove such compensating errors in models, not only to bring both the longwave and shortwave components on the cloud radiative effect into agreement with the observed values, but also because they must be associated with errors in the vertical profile of cloud radiative heating, particularly in the longwave, as discussed in Slingo et al. (1998). These problems also demonstrate the need for independent information on cloud overlaps and cloud vertical structure, which the new generation of active satellite sensors promise.

In the cases examined here, compensations between different cloud types that lead to the models having the right cloud radiative effect in a particular region are more common in the shortwave than in the longwave. This is probably because there is less of a strong contrast between the cloud radiative effect between typical low, midlevel and high top dominant events in the shortwave than the longwave, making it easier for low clouds to compensate for a lack of mid-level or high top cloud in the shortwave than in the longwave.

Possible causes of these model problems have been suggested and merit further investigation. The different amounts of cloud with mid-level tops visible from above in the mid-latitudes may be due to the differing treatments of cloud overlap and/or convection in the LMD versus the Hadley Centre and ECMWF models. It is interesting to note that while the LMD and Hadley Centre models have the most similar large-scale cloud schemes, it is the Hadley Centre and ECMWF models whose errors in this region look similar.

Analysis of the models' abilities to simulate the observed relationship between daily mean cloud amount, albedo and OLR suggests that there are a number of problems in the three models which are likely to affect their ability to simulate a simple 'cloud amount' type feedback. However, most of the features of the observed relationships are reproduced well by at least one model, which is hopeful as it suggests that a good all round simulation of these relationships should be achievable in a single model if sufficient analysis of the model differences is undertaken. It also demonstrates a clear benefit of using multiple models in observationally based model validation studies.

Two distinct types of cloud feedback have been discussed here. While there is reason to doubt that current models are able to simulate potential 'cloud regime' type feedbacks with skill, there is hope that a model capable of simulating potential 'cloud amount' type feedbacks will be achievable once the reasons for the remaining differences between the models are understood. Improvements in the simulation of clouds in stratocumulus, trade cumulus and deep convective regimes would be likely to have a positive effect on the former problem.

For future work, it is foreseen that the link between modelled cloud feedbacks, cloud parametrisations and observed cloud behaviour could be strengthened by combining the techniques presented here with those currently used to examine the sensitivity of observed cloud radiative effect to SST, for example the technique of Bony et al. (1997), in which the relationships between clouds and SST are examined in various dynamical regimes of 500 hPa vertical velocity. Such relationships can be thought of as 'proxies' for cloud feedbacks under climate change. Analysis of the same three climate models presented here (Bony personal communication) shows that none of the models studied correctly captures the relationships in all dynamical regimes and so, if it is the case that the proxies accurately reflect cloud feedbacks, the models will all have difficulty representing the clouds in a future climate. The application of the techniques demonstrated in this study in a similar manner would enable a more detailed study of these model limitations and give concrete examples of model problems that lead to unrealistic cloud feedbacks. If this is achieved, it will be possible to rank model problems in terms of their impact on the simulation of cloud feedback, and so to focus development on those areas where model improvements are most likely to reduce the uncertainty.

A further challenge will be to develop techniques to allow the links between clouds and the larger hydrological cycle to be thoroughly tested in climate models; the extent to which the errors in the cloud distributions in models are caused by problems with moisture transports (for instance from boundary layer and convective mixing) is not currently clear, although some of the results presented here suggest that some systematic errors in the

cloud distribution may be less sensitive to the choice of cloud scheme than to the choice of convection scheme.

Acknowledgements The work at the Hadley Centre study was funded by the UK Department of Environment, Transport and the Regions, under contract PECD 7/12/37. The model runs and travel costs for the collaboration were supported by a European Community funded project on Cloud Feedbacks and Validation. The ISCCP and ERBE data were obtained from the NASA Langley Research Center EOSDIS Distributed Active Archive Center. The authors are grateful to Steve Klein for making code available which was used here in a modified form, and to Roy Kershaw and Tony Slingo for their helpful comments on the manuscript.

References

Barker HW (1996) A parameterization for computing grid-averaged solar fluxes for inhomogeneous marine boundary layer clouds. Part I. Methodology and homogeneous biases. J Atmos Sci 53: 2289–2303

Bony S, Lau K-M, Sud YC (1997) Sea surface temperature and large-scale circulation influences on tropical greenhouse effect and cloud radiative forcing. J Clim 10: 2055–2077

Cess RD, Potter GL, Blanchet JP, Boer GJ, Del Genio AD, Deque M, Dymnikov V, Galin V, Gates WL, Ghan SJ, Kiehl JT, Lacis AA, Le Treut H, Li ZX, Liang XZ, Macavaney BJ, Meleshko VP, Mitchell JFB, Morcrette J-J, Randall DA, Rikus L, Roeckner E, Royer JF, Schelse U, Scheinin DA, Slingo A, Sokolov AP, Taylor KE, Washington WM, Wetherald RT, Yagai I, Zhang MH (1990) Intercomparison and interpretation of climate feedback processes in 19 atmospheric general circulation models. J Geophys Res 95: 16 601–615

Chen T, Rossow WB, Zhang Y (2000) Radiative effects of cloud-type variations. J Clim 13: 264–286

Cullen MJP (1993) The unified forecast/climate model. Meteorol Mag 122: 81–94

Cusack S, Edwards JM, Kershaw R (1999) Estimating the subgrid variance of saturation, and its parametrization for use in a GCM cloud scheme. Q J R Meteorol Soc 125: 3057–3076

Del Genio AD, Yao MS, Kovari W, Lo KKW (1996) A prognostic cloud water parameterization for global climate models. J Clim 9: 270–304

Doutriaux-Boucher M, Seze G (1998) Significant changes between the ISCCP C and D cloud climatologies. Geophys Res Lett 25: 4193–4196

Fouquart Y, Bonnel B (1980) Computations on solar heating of the Earth's atmosphere: a new parametrization. Beitr Phys Atmos 53: 35–62

Gregory JM (1999) Representation of the radiative effect of convective anvils. Hadley Centre Technical Note 7, Hadley Centre for Climate Prediction and Research, Meteorological Office, Bracknell, RG12

Harrison EF, Minnis P, Barkstrom BR, Ramanathan V, Cess R, Gibson GG (1990) Seasonal variation of cloud radiative forcing derived from the Earth Radiation Budget Experiment. J Geophys Res 95: 18 687–703

Heymsfield AJ, Donner LJ (1990) A scheme for parametrizing ice-cloud water content in general circulation models. J Atmos Sci 47: 1865–1877

Hortal M, Simmons AJ (1991) Use of reduced gaussian grids in spectral models. Mon Weather Rev 119: 1057–1074

Jakob C (1994) The impact of the new cloud scheme on ECMWF's integrated forecasting system. Proc ECMWF Workshop on Modelling, Validation and Assimilation of Clouds, Reading, UK, 31 Oct–4 Nov 19 277–294

Kattenberg A, Giorgi F, Grassl H, Meehl GA, Mitchell JFB, Stouffer RJ, Tokioka T, Weaver AJ, Wigley TML (1996) Climate models – projections of future climate. In: Houghton JT, Meira Filho LG, Callander BA, Harris N, Kattenberg A, Maskell K (eds), Climate change 1995. The science of climate change, Cambridge University Press, Cambridge, UK, pp 285–358

Klein SA, Jakob C (1999) Validation and sensitivities of frontal clouds simulated by the ECMWF model. Mon Weather Rev 127: 2514–2531

Kristjánsson JE, Edwards JM, Mitchell DL (1999) A new parameterization scheme for the optical propeties of ice crystals for use in general circulation models of the atmosphere. Phys Chem Earth 24: 231–236

Le Treut H, Li ZX (1991) Sensitivity of an atmospheric general circulation model to prescribed SST changes: feedback effects associated with the simulation of cloud optical properties. Clim Dyn 5: 175–187

Li ZX (1999) Ensemble atmospheric GCM simulation of climate interannual variability from 1979 to 1994. J Clim 12: 986–1001

Lock AP (1998) The parametrization of entrainment in cloudy boundary layers. Q J R Meteorol Soc 124: 2729–2753

Martin GM, Bush MR, Brown AR, Lock AP, Smith RNB (2000) A new boundary layer mixing scheme. Part II: Tests in climate and mesoscale models. Mon Weather Rev 128: 3200–3217

Morcrette J-J (1991) Radiation and cloud radiative properties in the ECMWF operational weather forecast model. J Geophys Res 96D: 9121–9132

Morcrette J-J (1993) Revision of the clear-sky and cloud radiative properties in the ECMWF model. ECMWF Newsl 61: 3–14

Pope VD, Gallani ML, Rowntree PR, Stratton RA (2000) The impact of new physical parametrizations in the Hadley Centre Climate Model: HadAM3. Clim Dyn 16: 123–146

Pope VD, Pamment JA, Jackson DR, Slingo A (2001) The representation of water vapour and its dependence on vertical resolution in the Hadley Centre Climate Model. J Clim (in press)

Roeckner E, Schlese U, Biercamp J, Leowe P (1987) Cloud optical depth feedbacks and climate modelling. Nature 329: 138–140

Rossow WB, Schiffer RA (1991) ISCCP cloud data products. Bull Am Meteorol Soc 72: 2–20

Rutledge SA, Hobbs PV (1983) The mesoscale and microscale structure and organization of clouds and precipitation in midlatitude cyclones. Part VIII. A model for the 'seeder-feeder' process in warm-frontal rainbands. J Atmos Sci 40: 1185–1206

Senior CA (1998) Comparison of mechanisms of cloud-climate feedbacks in GCMs. J Clim 12: 1480–1489

Senior CA, Mitchell JFB (1993) Carbon dioxide and climate: the impact of cloud parameterization. J Clim 6: 393–418

Slingo A, Pamment JA, Webb MJ (1998) A 15-year simulation of the clear-sky greenhouse effect using the ECMWF re-analyses: fluxes and comparisons with ERBE. J Clim 11: 690–708

Slingo A (1990) Sensitivity of the Earth's radiation budget to changes in low clouds. Nature 343: 49–51

Tiedtke M (1989) A comprehensive mass-flux scheme for cumulus parameterization in large-scale models. Mon Weather Rev 117: 1779–1800

Tiedtke M (1993) Representation of clouds in large-scale models. Mon Weather Rev 121: 3040–3061

Tiedtke M (1996) An extension of cloud-radiation parameterization in the ECMWF model: the representation of sub-grid scale variations of optical depth. Mon Weather Rev 124: 745–750

Wilson DR, Ballard SP (1999) A microphysically based precipitation scheme for the UK Meteorological Office Unified Model. Q J R Meteorol Soc 125: 1607–1636

Wood R, Field PR (2000) Relationships between total water, condensed water, and cloud fraction in stratiform clouds examined using aircraft data. J Atmos Sci 57: 1888–1905

Yu W, Doutriaux M, Seze G, Le Treut H, Desbois M (1996) A methodology study of the validation of clouds in GCMs using ISCCP satellite observations. Clim Dyn 12: 389–401